Ultrasound in Med. & Biol., Vol. 32, No. 4, pp. 569–577, 2006

0301-5629/06/$–see front matter

ELSEVIER

doi:10.1016/j.ultrasmedbio.2006.01.002

● *Original Contribution*

HIGH FREQUENCY NONLINEAR SCATTERING FROM A MICROMETER TO SUBMICROMETER SIZED LIPID ENCAPSULATED CONTRAST AGENT

DAVID E. GOERTZ,*† MARTIJN E. FRIJLINK,* NICO DE JONG,*†‡ and A. F. W. VAN DER STEEN*†

*Biomedical Engineering Department, Erasmus Medical Centre, Rotterdam, The Netherlands; †Interuniversity Cardiology Institute of The Netherlands, Utrecht, The Netherlands; and ‡Physics of Fluids, University of Twente, Enschede, The Netherlands

(*Received* 11 *July* 2005; *revised* 27 *December* 2005; *in final form* 5 *January* 2006)

Abstract—An experimental lipid encapsulated contrast agent comprised substantially of micrometer to submicrometer diameter bubbles was evaluated for its capacity to produce nonlinear scattering in response to high transmit frequencies. Agent characterization experiments were conducted at transmit frequencies of 20 and 30 MHz with bandwidths of 5, 15 and 25% using a broadband focused PVDF transducer. The presence of subharmonic energy was observed for all bandwidths at a wide range of pressures (0.49 to 5.7 MPa and 0.45 to 4.5 MPa for the 20 and 30 MHz cases, respectively). Distinct ultraharmonics were observed only in the 5% bandwidth cases. Second harmonic energy was also present, but this was at least partly due to nonlinear propagation, as indicated by linear scatterer signals. Evidence of destruction was found only at higher peak negative pressures (*e.g.*, >2 MPa for 30 MHz 5% bandwidth pulse). The results suggest that small lipid bubble formulations may be useful for the purposes of high frequency nonlinear contrast imaging.
(E-mail: d.goertz@erasmusmc.nl)

Key Words: **High frequency, Intravascular ultrasound, Harmonic, Nonlinear, Contrast agents, Microbubbles.**

INTRODUCTION

There is a growing interest in the use of microbubble contrast agents at transmit frequencies above 15 MHz. One motivation is to conduct high frequency molecular imaging with targeted contrast agents. A second is to improve the performance of high frequency microvascular flow imaging systems. The majority of reports to date have examined or assumed linear microbubble scattering at high transmit frequencies. Deng et al. (1998) reported imaging and spectral analysis of Albunex™ (Molecular Biosystems Inc., San Diego, CA, USA) at 40 MHz. Cachard et al. (1997) conducted phantom experiments using Echovist™ (Shering, Berlin, Germany) and found improvements in lumen boundary detection using 30 MHz intravascular ultrasound (IVUS). Moran et al. (2002) measured the backscattered power from four commercial contrast agents using IVUS instrumentation. A number of studies have examined experimental liposomal dispersions comprised of lipid encapsulated air bubbles with number mean diameters of below 1 μm, with a view for use in molecular imaging (*e.g.*, Demos et al. 1999; Huang et al. 2002). Demos et al. (1999) employed such targeted echogenic liposomes to detect thrombus *in vivo* through an enhancement of IVUS echogenicity. Moran et al. (2004) measured the backscattered power from an in-house liposomal agent at 40 MHz.

The success of contrast imaging at lower ultrasound frequencies (2 to 5 MHz) has been largely due to the ability to initiate and detect nonlinear microbubble signals (*e.g.*, Goldberg et al. 2001; Becher and Burns 2000). Although not designed for use at high frequencies, it has been shown that Definity™ (Bristol-Myers Squibb Medical Imaging, New York, NY, USA) can be stimulated to produce substantial amounts of nonlinear scattering at transmit frequencies (f_{trans}) of at least up to 32 MHz (Goertz et al. 2001). At 20 MHz for example (15% −6 dB bandwidth Gaussian enveloped pulses), the transmit pressure was varied between 1.1 and 7.8 MPa and subharmonic, ultraharmonic and second harmonic energy was found to be present at all pressure levels. This work

Address correspondence to: David Goertz, Biomedical Engineering, Erasmus Medical Centre, Room EE2302, Dr. Molewaterplein 50, 3015 GE Rotterdam, The Netherlands. E-mail: d.goertz@erasmusmc.nl

was extended to show the feasibility of nonlinear imaging at transmit frequencies of up to 30 MHz (Goertz et al. 2005a) with Definity™. In this study, the relative (−12 dB) transmit bandwidths at 20 MHz were 17, 27 and 34%, and peak negative pressures were varied between 0.5 and 3 MPa. Subharmonic imaging was demonstrated for transmit frequencies of 20 and 30 MHz and ultraharmonic imaging for a 20 MHz transmit frequency. Second harmonic imaging for a 20 MHz transmit frequency was not found to improve contrast to tissue ratios (CTR) due to the presence of strong tissue propagation harmonics under the conditions investigated.

It has been hypothesized that nonlinear scattering observed for current commercial agents at higher transmit frequencies is associated with a subpopulation of smaller bubbles. The application of existing encapsulated bubble models suggests that bubbles of diameters below 1 to 2 μm may be active in a nonlinear manner for transmit frequencies above 15 MHz (Goertz et al. 2003), although the validity of such models and shell properties have yet to be determined at high frequencies. Optical observations using a fast frame camera (Goertz et al. 2004) have found evidence of bubble sizes on the order of 1.8 μm and below undergoing subharmonic oscillations in response to 19 MHz transmit pulses. Further, mechanical filtration experiments that preferentially isolated subpopulations of bubbles below 1 to 2 μm in diameter from BR14 (Bracco Research, Geneva, Switzerland) indicated that harmonic to fundamental frequency signal ratios were improved at 20 and 30 MHz transmit frequencies (Goertz et al. 2003). For example, at a 30 MHz transmit frequency, the application of a 1 μm filter improved the second harmonic to fundamental frequency ratio by 8 dB and the subharmonic to fundamental frequency ratio by 11 dB.

The objective of this study was to investigate the feasibility of producing nonlinear scattering from a contrast agent (BG2423, Bracco Research, Geneva, Switzerland) comprised substantially of micrometer and submicrometer bubbles using high transmit frequencies. Agent characterization experiments were conducted as a function of pressure and bandwidth for transmit frequencies of 20 and 30 MHz. The first type of experiment was to measure the scattering response from the agent. A second experiment tested for bubble disruption by repeatedly pulsing a group of bubbles.

METHODS

Agent characterization experiments were performed using a broadband focused PVDF transducer (f-number 1.6; aperture 8 mm; center frequency 19 MHz). This transducer afforded the opportunity to employ 20 and 30 MHz transmit pulses for a range of bandwidths with a controlled pressure at focus. The experiments were conducted using a flow cell apparatus similar to that described in Goertz et al. (2003, 2005a). The transducer beam was passed into the flow cell through a mylar membrane oriented at 80 degrees with respect to the beam axis. The focus of the transducer was situated 1.8 mm behind the membrane. An arbitrary waveform generator (Lecroy LW420A, Chestnut Ridge, NY, USA) was used to generate low amplitude pulses, which were amplified with a 60-dB gated linear power amplifier (LPI-10, ENI, Rochester, NY, USA) and then bandpass filtered before being sent to the transducer. The bandpass filters employed were custom-made 5th order Butterworth (12 to 28 MHz −3dB for 20 MHz f_{trans}; 22 to 42 MHz −3 dB points for 30 MHz f_{trans}) which reduced the transmitted second harmonic signal levels to at least 42 dB below the fundamental frequency and eliminated the effects of power amplifier gating. On receive, the RF signals were amplified with a 35 dB preamplifier (AU-1189 Miteq, Hauppage, NY, USA), and bandpass filtered with a custom 3rd order Butterworth filter (12 to 60 MHz −3 dB points). The signals were then digitized at 200 mega samples/s with a PC based 8-bit A/D PCI-card (DP235, Acqiris, Geneva, Switzerland).

All spectra were calculated within a 2 μs window around the geometric focus, after the application of a Hanning window. Noise-only acquisitions were made with the transmit pulse off, and the reported scattering results have had the noise spectra subtracted. The results have not been compensated for the transducer frequency response, to provide an indication of the relative signal levels available for imaging in each nonlinear frequency band. For the purposes of comparison, the spectra have been normalized with respect to the maximum fundamental frequency energy for each bandwidth.

The contrast agent employed was BG2423 (Bracco Research), an experimental lipid encapsulated formulation comprised substantially of micrometer and submicrometer bubbles. Further details of the size distribution cannot be disclosed due to proprietary considerations. The agent was diluted in saline (0.9% NaCl by weight) by a factor of 1000 times relative to that in the vial. Solid particles, which were assumed to have linear scattering characteristics, were also employed to assess the presence of nonlinear propagation or energy transmitted outside of the intended bandwidth. Following a procedure similar to that described in Ramnarine et al. (1998), the scatterer suspension was comprised of 5 μm polyamide particles (2001USNAT1, Orgasol™, ELF Autochem, Paris, France) mixed with distilled water at a concentration of 2% by weight, with 1% Triton X-100 (Sigma-Aldrich, St. Louis, MO, USA) added to inhibit the aggregation of particles. In Ramnarine et al. (1998), these particles were evaluated at a transmit frequency of 5

Table 1. Summary of measured relative transmit bandwidths employed in the agent characterization experiments

Transmit center frequency	20 MHz			30 MHz		
Nominal −6 dB input BW	5%	15%	25%	5%	15%	25%
−6 dB meas. BW	5%	16%	27%	5%	15%	26%
−12 dB meas. BW	7%	22%	38%	7%	24%	34%
−12 dB meas. freq. range (MHz)	19.3–20.7	17.7–22.1	16.0–23.7	28.9–31.0	26.0–33.2	24.1–34.3

MHz, although these particles have also been employed at a frequency of 28 MHz (Gatzoulis et al. 2003).

The first type of experiment performed was to assess the scattering response from the agent in pulse-echo mode. This was accomplished while agent was flowing through the beam at a rate that permitted replenishment within the focal zone between pulses (sent at 0.5 Hz). Averages of 80 independent received traces are reported from two vials of agent. Experiments were conducted as a function of bandwidth (nominal 5, 15, 25% −6 dB input bandwidths) and pressure using Gaussian enveloped pulses at center frequencies of 20 or 30 MHz. In these experiments, both contrast agent and linear scatterers were assessed. Noise-only data were acquired with the AWG transmit power off.

For the 30 MHz 5% transmit bandwidth case, these data were quantified by integrating the power in four different frequency bands: subharmonic (0.4 to 0.6 f_{trans}), fundamental (0.9 to 1.1 f_{trans}), ultraharmonic (1.4 to 1.6 f_{trans}) and second harmonic (1.9 to 2.1 f_{trans}). Mean and standard deviations of these data were calculated in the log domain, and all data were normalized with respect to the fundamental frequency power of the contrast agent at maximum transmit amplitude. Noise-only mean powers were also calculated and displayed.

The second type of experiment was to test for agent destruction by sending a sequence of 250 pulses at 2 kHz under no-flow conditions. Between acquisitions, fresh agent was brought within the focal zone and was permitted to stabilize for approximately 10 s to avoid motion effects before pulses were sent. Results are reported for a 30 MHz transmit frequency at 5 and 25% bandwidths.

Pressures and bandwidths were measured in water tank hydrophone experiments with a 0.075 mm needle hydrophone (Precision Acoustics Ltd., Dorchester, UK) situated at the transducer focus. The measured transmit −6 dB and −12 dB relative bandwidths and −12 dB frequency ranges (at the lowest pressure levels) are summarized in Table 1. Peak negative pressures are reported. For the 5% bandwidth agent acquisitions, a total of six pressures were used ranging from 0.27 to 5.7 MPa for 20 MHz and 0.24 to 4.5 MPa for 30 MHz. For the 15 and 25% bandwidth agent acquisitions and all linear scatterer acquisitions, only five pressure levels were employed (from 0.49 to 5.3 MPa and 0.47 to 4.5 MPa for the 20 and 30 MHz cases, respectively) due to signal to noise ratio (SNR) issues at the lowest transmit level. The peak negative pressure values and mechanical indices (MI) are shown in Table 2 for the 30 MHz 5% bandwidth case. MI was calculated as the peak negative pressure over the square root of the transmit center frequency in MHz. While the absolute pressure values employed are high relative to those used at lower diagnostic ultrasound frequencies, it can be observed that the MI ranges do overlap considerably. Further, a clinical IVUS system operating at a nominal center frequency of 30 MHz was reported to operate with a peak negative pressure of 3.27 MPa (MI = 0.59) (Moran et al. 2002).

RESULTS

Scattering results for the agent and linear scatterers at a transmit frequency of 20 MHz are shown in Fig. 1. A pressure dependent transmit frequency peak was present for all bandwidths and pressures for both the contrast agent and linear scatterers. As the pressure was increased, second harmonic signals (40 MHz) could also be observed from the agent and linear scatterers, the latter indicating the presence of nonlinear propagation. A peak can also be observed at half the transmit frequency (10 MHz) for the agent. This is referred to as the (order one half) subharmonic frequency, since energy has been coupled into half the transmit frequency. For the 5% bandwidth case, but not the 15 or 25% cases, a distinct ultraharmonic peak (at 30 MHz for the 2.0 MPa case) can be discerned. For all bandwidths, the highest transmit pressure levels employed produced broadband scattered energy, which has previously been observed in conditions where bubble destruction is occurring (Uhlendorf and Hoffman 1994). It should be noted that significant scattered energy outside the transmit and second harmonic frequencies was not in general observed with the linear scatterers, supporting the conclusion that the energy in these frequency bands was associated with nonlinear scattering in the case of the agent.

Table 2. Summary of measured peak negative pressures and mechanical indices for the 30 MHz 5% bandwidth case

Pressure (MPa)	0.24	0.49	0.81	1.8	2.8	4.5
MI	0.04	0.09	0.15	0.33	0.51	0.82

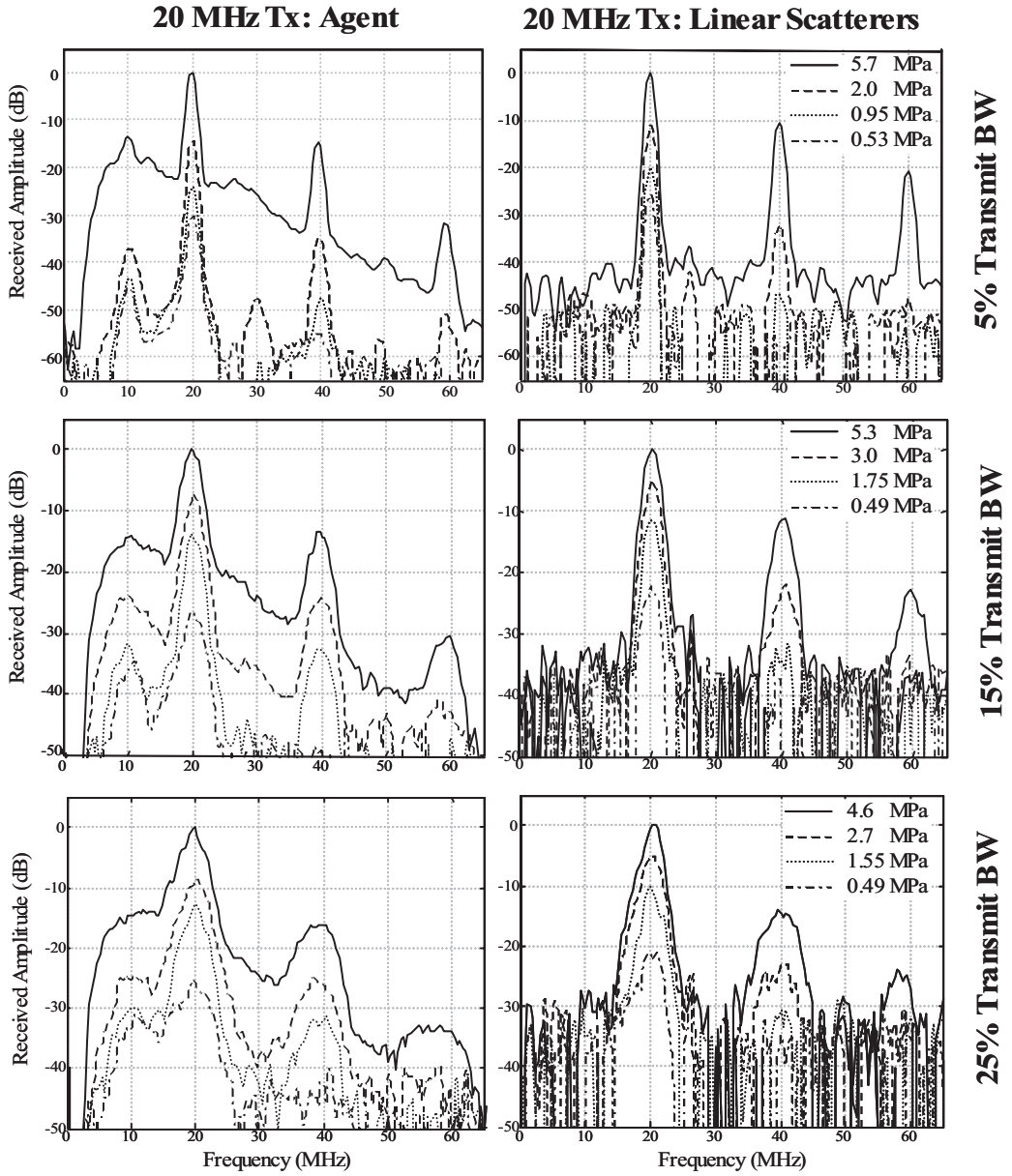

Fig. 1. Normalized received spectra from agent (left column) and linear scatterers (right column) for 20 MHz pulses as a function of transmit amplitude (peak negative pressures specified). Transmit bandwidths of 5% (top), 15% (middle) and 25% bottom are shown. For the linear scatterers, energy is present in the transmit frequency band and, at higher pressures, in the second harmonic frequency region (40 MHz). For the agent, energy can be coupled into the subharmonic (10 MHz), ultraharmonic (30 MHz) and second harmonic (40 MHz).

The scattering results for a 30 MHz transmit frequency, shown in Fig. 2, exhibited a similar pattern to the 20 MHz results. Clear fundamental, subharmonic and second harmonic energy can be observed for all bandwidths investigated for the agent. Distinct ultraharmonics were evident only for the 5% bandwidth case. For all bandwidths, the highest pressures employed result in broad bandwidth signals.

A quantification of the results for the 30 MHz 5% bandwidth case is shown in Fig. 3. For the fundamental frequency, a monotonic increase in received energy was observed as a function of pressure for both contrast and linear scatterers. For the subharmonic agent signals, three pressure ranges can be identified. At the lowest pressure employed (0.24 MPa), no significant subharmonic signal was detectable above the noise floor, due to either its absence or to poor SNR. By 0.5 MPa, the subharmonic has undergone a rapid growth, and then increases slowly until 1.9 MPa. After this point there is an increase in growth rate for the two highest pressures.

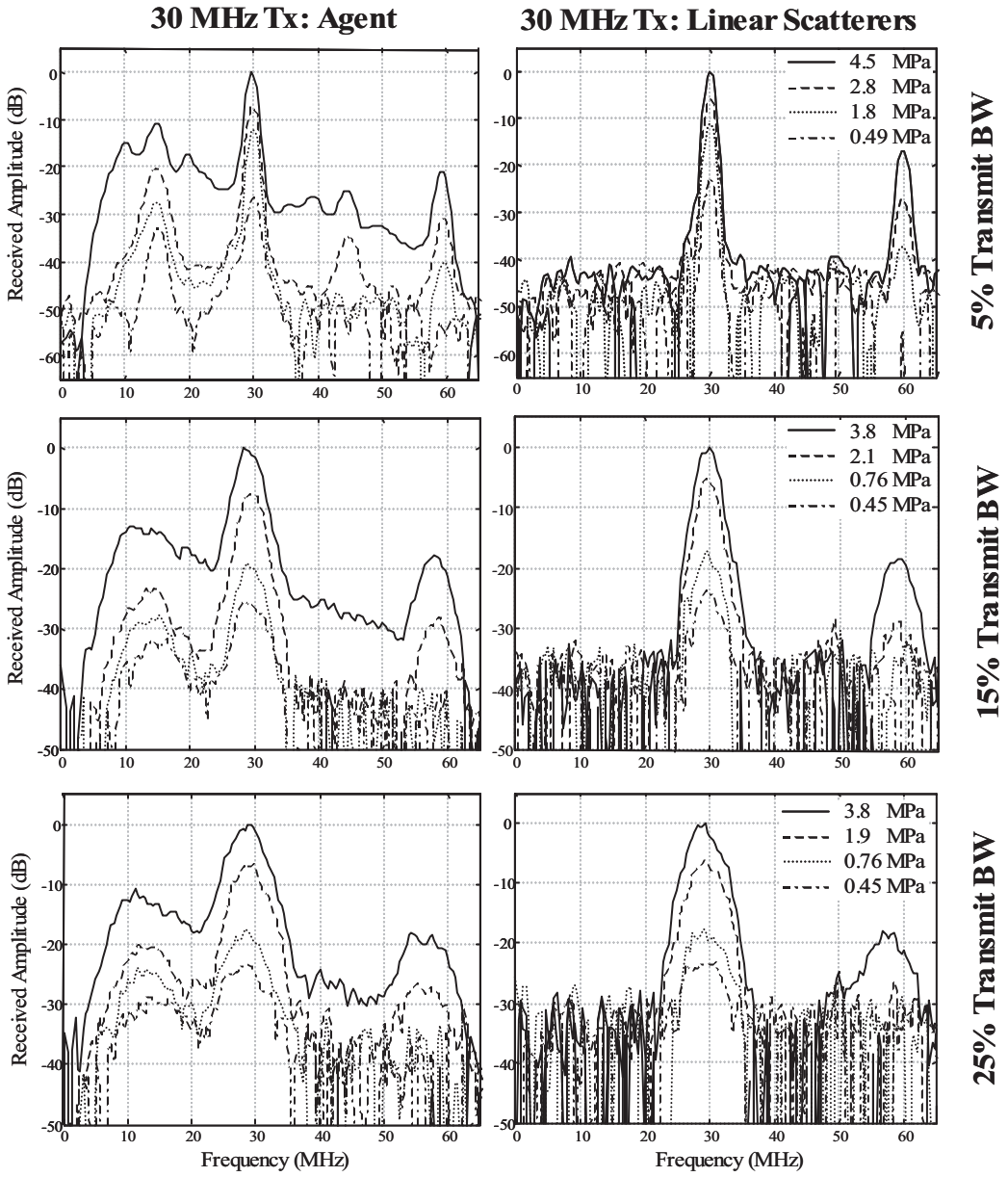

Fig. 2. Normalized received spectra from agent (left column) and linear scatterers (right column) for 30 MHz pulses as a function of transmit amplitude (peak negative pressures specified). Transmit bandwidths of 5% (top), 15% (middle) and 25% (bottom) are shown. For the linear scatterers, energy is present in the transmit frequency band and, at higher pressures, in the second harmonic frequency region (60MHz). For the agent, energy has been coupled into the subharmonic (15 MHz), ultraharmonic (45 MHz) and second harmonic (60 MHz).

The linear scatterer subharmonic frequency data were significant only at the highest pressure levels, where energy leakage of the transmitted pulse has occurred. In the ultraharmonic region, contrast agent energy exceeds the linear scatterer energy only at the highest two pressure levels. The second harmonic power for both agent and linear scatterers follows a similar pattern, and is not significantly above the noise floor at the lower transmit amplitudes.

Example destruction results are shown in Fig. 4 for a 30 MHz transmit frequency. For the 5% bandwidth case (top left), the highest pressure employed (4.5 MPa) has resulted in distinct peaks at the fundamental (F30–30 MHz center), subharmonic (SH15–15 MHz center), and second harmonic (H60–60 MHz center) regions. Additionally, it resulted in broadband energy within the first 20 to 25 pulses (~10 to 12 ms). This is consistent with the "first-pulse" spectral data observed in Fig. 2, which

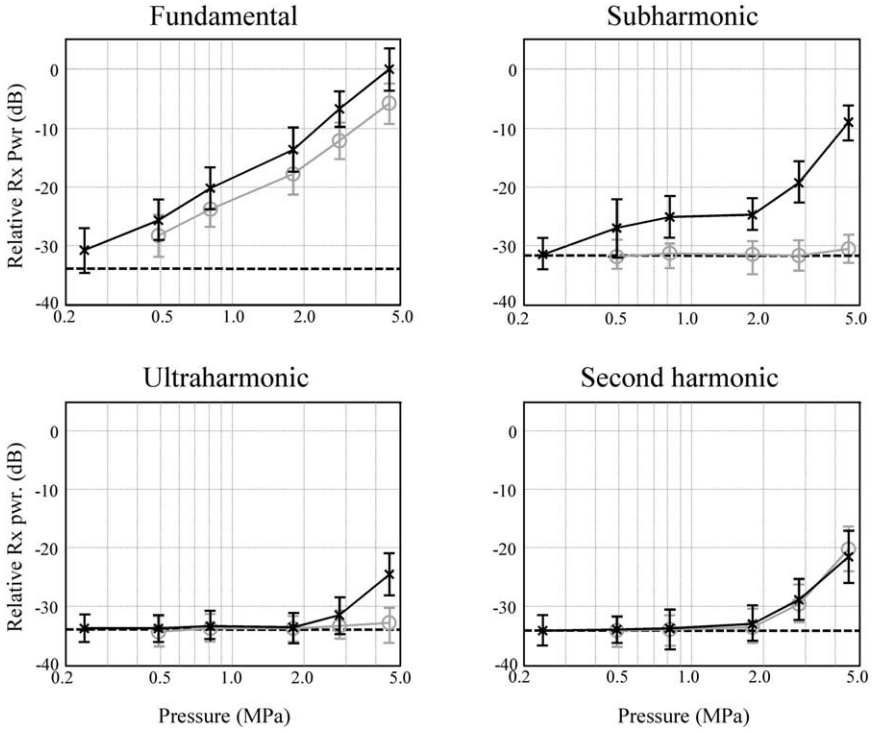

Fig. 3. Quantified 30 MHz scattering data as a function of peak negative transmit pressure for agent (x) and linear scatters (o). Noise floors are indicated with dashed lines. Normalized (with respect to fundamental frequency at maximum transmit amplitude) received power is shown for fundamental (24 to 36 MHz), subharmonic (9 to 21 MHz), ultraharmonic (39 to 51 MHz) and second harmonic (54 to 66 MHz) frequencies.

showed broadband energy present alongside peaks at F30, SH15 and H60. Following these initial pulses, the broadband energy diminishes, and the remaining energy is then present only in distinct subharmonic, fundamental and second harmonic frequency bands. This is attributed to the destruction of at least a portion of the bubbles present within the focal zone during the first 20 to 25 pulses. The remaining energy after this point may be associated with either bubbles that were originally present and not destroyed, or with ones that have moved into the focal zone due to the effects of radiation pressure. As the transmit pressure was decreased to 1.8 MPa (top right), the presence of broadband energy was not observed. These data indicate that nondestructive subharmonic generation is occurring at this pressure level. Note that this pressure corresponds to the endpoint of the slowly growing subharmonic pressure range (Fig. 3), whereas the higher pressure level (4.5 MPa) corresponds to the second rapid growth region for the subharmonic. One interpretation of this is that the increases in subharmonic energy at the highest pressure is at least in part the result of bubble destruction.

A qualitatively similar pattern is observed for the 25% bandwidth case. At the highest pressure of 3.4 MPa (bottom left), fundamental (F30), subharmonic (SH15) and second harmonic (H60) energy can be observed. Broadband energy is also present within the first 100 pulses, consistent with the occurrence of destruction. The longer period of apparent bubble destruction relative to the 5% bandwidth case may be attributable to the reduced energy present in the shorter 25% bandwidth pulses, as well as the lower pressure level achieved with these pulses (3.4 MPa versus 4.5 MPa). As the pressure is reduced to 1.9 MPa (bottom right), the destruction pattern is not evident.

DISCUSSION AND CONCLUSIONS

Previous studies have indicated that nonlinear scattering observed in conventional agents at high frequencies (>15 MHz) may be associated with a subpopulation of small bubbles (<1 to 2 micrometers). Bubbles of this size account for only a small portion of the volume fraction of current commercial agents (*e.g.*, Unger et al. 1994; Gorce et al. 2000), This implies that the large majority of the volume fraction of such agents may not be contributing significantly to nonlinear signals stimulated by high transmit frequencies. The present study has demonstrated that nonlinear scattering is possible for transmit frequencies in the 20 to 30 MHz range using a

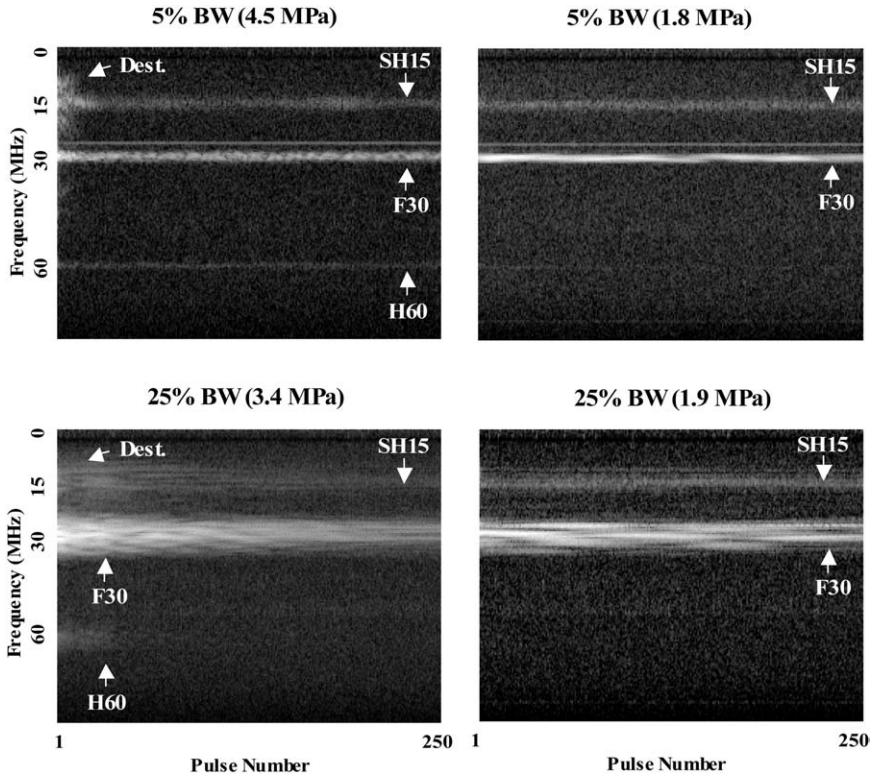

Fig. 4. Destruction experiments for 30 MHz transmit pulses examine spectra as a function of successive pulses. At 4.5 MPa and a 5% transmit bandwidth (top left), broadband energy is emitted in response to the first 20 to 25 pulses (labeled "Dest."), consistent with the destruction of at least a portion of the agent. Following this, distinct subharmonic (SH15), fundamental (F30) and second harmonic (H60) signals can be observed. When the pressure is reduced to 1.8 MPa (top right) this pattern does not occur, although subharmonic (SH15) and fundamental (F30) signals are present. Note that a sharp peak is also present at 26 MHz, which is associated with system noise on receive. A similar pattern is observed for the 25% bandwidth case at the highest (3.4 MPa, bottom left) and reduced pressure (1.9 MPa, bottom right).

contrast agent comprised primarily of micrometer to submicrometer sized bubbles. This result indicates that the use of smaller bubble populations may be appropriate for nonlinear imaging at high transmit frequencies. It should be emphasized, however, that a quantitative comparison of nonlinear scattering as a function of size has not been made, and, as such it, cannot be concluded that the bubbles employed in this study are optimal for high frequency nonlinear imaging.

The ability to initiate subharmonics from contrast agents has been previously demonstrated at both low frequencies (*e.g.*, Lotsberg et al. 1996; Shankar et al. 1999; Shi et al. 1999b; Shi and Forsberg 2000) and high frequencies (Goertz et al. 2001; 2005a). The results of the present study have indicated a lower pressure region of subharmonic growth or onset (<0.5 MPa), followed by a period of slow growth (~0.5 to 2 MPa) and a third region of more rapid growth (>2 MPa). An onset pressure level for detectible subharmonics was not observed in previous experiments conducted with Definity™ at 20 MHz. This may be because these studies did not employ a sufficiently low pressure to observe this (>0.5 MPa in Goertz et al. 2005a; >1.1 MPa in Goertz et al. 2001), or to differences in agent properties. The intermediate pressure region produced subharmonics without detectible disruption. The possibility of nondestructive subharmonics generation has been previously reported at lower frequencies (Shi et al. 1999a; Chomas et al. 2001), and is consistent with a report of coherent subharmonic velocity imaging with Definity™ at a 20 MHz transmit frequency (Goertz et al. 2005b). Finally, destruction experiments indicated the presence of bubble disruption in the highest pressure region where growth is rapid. This was also observed with Definity™ at 20 MHz (Goertz et al. 2001).

At a transmit frequency of 2 MHz, Shi and Forsberg (2000) also identified three stages of subharmonic generation. The first was when subharmonics were present but low in amplitude ("insignificant") and slowly growing. The second was one of rapid growth. The third was saturation, where the distinct subharmonic frequency peaks diminish in the presence of wide bandwidth emis-

sions related to bubble disruption, although this was not explicitly examined. A direct comparison with these data is complicated by the limited number of pressures employed. However, the results are not inconsistent with each other, particularly when considering that the delineation between possible regions may be diffuse. Specifically, the slow and rapidly growing stages may occur in both cases, while a saturation phase may not be evident in the present study because of a limited pressure range. An onset threshold for subharmonics was not observed by Shi and Forsberg (2000), although this may be due to insufficiently low pressures being employed. Alternatively, it is conceivable that different agents (albumin encapsulated Optison™ versus a lipid encapsulated small bubble agent) and transmit frequencies result in different forms of pressure dependence for subharmonic generation.

The results have indicated that significant ultraharmonic energy is not detected until higher transmit pressures (>2 MPa) and is generally not in the form of a distinct peak. The exception to this was the 20 MHz 5% bandwidth transmit case. These findings are consistent with those of Goertz et al. (2005a), where it was found that ultraharmonic imaging did not result in substantial contrast to noise ratios until pressures greater than 2 MPa.

For second harmonic signals, a strong propagation harmonic was also present, and an enhancement of second harmonic agent scattering relative to linear scatterers was not evident. A propagation second harmonic was also observed with PVDF transducers at a 20 MHz transmit frequency by Cherin et al. (2002) and Goertz et al. (2005a). In the latter study, the propagation harmonic was prominent enough to degrade CTR in second harmonic imaging of Definity™ with a transmit frequency of 20 MHz. The relative CTR for the second harmonic signals will depend on tissue properties (scattering, attenuation and nonlinearity), as well as transmit conditions (beam diffraction and pressure level). In Goertz et al. (2006), second harmonic imaging is investigated with BG2423 using a prototype harmonic IVUS system, and the results indicate that at lower pressures ($\sim<0.3$ MPa), an improvement in CTR is possible to achieve.

Apart from their pronounced nonlinear activity at high frequencies, micrometer to submicrometer bubbles may be advantageous from the perspective of imaging microvessels at high spatial resolution. Assuming a given volume fraction of gas within an agent, a smaller mean bubble size will result in a larger number of bubbles per unit volume. This in turn may lead to a higher bubble number density in the blood stream, a factor that may be significant for high resolution imaging of the microvessels. Specifically, with high frequency applications that approach the scale of the microvasculature, the volume of blood potentially within the sample volume decreases accordingly and with it the probability that a bubble is present within the sample volume. Experiments are currently being conducted to evaluate the performance of the agent *in vivo*. While small bubble lipid encapsulated agents have been successfully employed *in vivo* in "linear" imaging modes (*e.g.*, Demos et al. 1999), their nonlinear behavior remains to be evaluated.

The results of this study suggest that nonlinear imaging of micrometer to submicrometer lipid agents may be useful for high frequency contrast imaging applications with ultrasound biomicroscopy and IVUS systems.

Acknowledgments—This work was financially supported by the Dutch Technology Foundation (STW). The authors thank S. Foster for providing the PVDF transducer. The agent was provided by Bracco Research (Geneva).

REFERENCES

Becher H, Burns PN. Handbook of contrast echocardiography. New York: Springer, 2000.

Cachard C, Finet G, Bouakaz A, Tabib A, Francon D, Gimenez G. Ultrasound contrast agents in intravascular echography: An *in vitro* study. Ultrasound Med Biol 1997;23:705–717.

Cherin EW, Poulsen JK, van der Steen AFW, Lim B, Foster FS. Experimental characterization of fundamental and second harmonic beams for a high-frequency ultrasound transducer. Ultrasound Med Biol 2002;28:635–646.

Chomas JE, Dayton P, Allen J, Morgan K, Ferrara KW. Mechanisms of contrast agent destruction. IEEE Trans Ultrason Ferroelec Freq Control 2001;48:232–248.

Demos SM, Alkan-Onyuksel H, Kane BJ, Ramani K, Nagaraj A, Greene R, Klegerman M, McPherson DD. *In vivo* targeting of acoustically reflective liposomes for intravascular and transvascular ultrasonic enhancement. J Am Coll of Cardiol 1999;33:867–875.

Deng CX, Lizzi FL, Silverman RH, Ursea R, Coleman DJ. Imaging and spectrum analysis of contrast agents in the *in vivo* rabbit eye using very high frequency ultrasound. Ultrasound Med Biol 1998;24:383–394.

Gatzoulis L, Ramnarine KV, Pye SD, Anderson T, Newby TE, Hoskins PR, McDicken WN. Doppler color flow imaging and flow quantification with a novel forward-viewing intravascular ultrasound system. Ultrasound Med Biol 2003;29:53–64.

Goertz DE, Wong SWS, Cherin E, Chin CT, Burns PN, Foster FS. Non-linear scattering properties of microbubble contrast agents at high frequencies. Proceedings of the IEEE Ultrasound Symposium, Atlanta, GA, 2001:1747–1750.

Goertz DE, Frijlink ME, Bouakaz A, Chin CT, de Jong N, van der Steen AFW. The effect of bubble size on nonlinear scattering at high frequencies. Proceedings of the IEEE Ultrasound Symposium, Honolulu, HI, 2003:1503–1507.

Goertz DE, Chin CT, Laan F, et al. Optical observations of microbubbles at high ultrasound frequencies. IEEE Ultrason Symp 2004 (abstract): 159–160.

Goertz DE, Cherin E, Needles A, et al. High frequency nonlinear b-scan imaging of microbubble contrast agents. IEEE Trans Ultrason Ferroelec Freq Control 2005a;52:65–79.

Goertz DE, Needles A, Burns PN, Foster FS. High frequency nonlinear color flow imaging of microbubble contrast agents. IEEE Trans Ultrason Ferroelec Freq Control 2005b;52:495–502.

Goertz DE, Frijlink ME, de Jong N, van der Steen AFW. Nonlinear intravascular ultrasound contrast imaging. Ultrasound Med Biol 2006;32:491–502.

Goldberg BB, Raichlen JS, Forsberg F, eds. Ultrasound contrast agents: Basic principles and clinical applications echocardiography, 2nd ed. London: Martin Dunitz, 2001.

Gorce JM, Arditi M, Schneider M. Influence of bubble size distribution on the echogenicity of ultrasound contrast agents—A study of SonoVue. Invest Radiol 2000;35:661–671.

Huang SL, Hamilton AJ, Pozharski E, et al. Physical correlates of the ultrasonic reflectivity of lipid dispersions suitable as diagnostic contrast agents. Ultrasound Med Biol 2002;28:339–348.

Lotsberg O, Hovem JM, Aksum B. Experimental observation of subharmonic oscillations of Infoson bubbles. J Acoust Soc Am 1996; 99:1366–1369.

Moran CM, Watson RJ, Fox KAA, McDicken WM. *In vitro* acoustic characterization of ultrasonic contrast agents at 30 MHz. Ultrasound Med Biol 2002;28:785–791.

Moran CM, Ross J, Cunningham C, Butler M, McDicken WM. *In vitro* 40 MHz ultrasonic characterization of in-house liposomal dispersions developed for targeting atherosclerotic plaque. Proceedings of the IEEE Ultrasound Symposium, Montreal, Quebec, Canada, 2004;1395–1398.

Ramnarine KV, Nassiri DK, Hoskins PR, Lubbers J. Validation of a New Blood-Mimicking Fluid for Use in Doppler Flow Test Objects. Ultrasound Med Biol 1998;24:451–459.

Shankar PM, Krishna PD, Newhouse VL. Subharmonic backscattering from ultrasound contrast agents. J Acoust Soc Am 1999;106:2104–2110.

Shi WT, Forsberg F, Hall AL, et al. Subharmonic imaging with microbubble contrast agents: Initial results. Ultrasonic Imaging 1999a;21:79–94.

Shi WT, Forsberg F, Raichlen JS, Needleman L, Goldberg BB. Pressure dependence of subharmonic signals from contrast microbubbles. Ultrasound Med Biol 1999b;25:275–283.

Shi WT, Forsberg F. Ultrasonic characterization of the nonlinear properties of contrast microbubbles. Ultrasound Med Biol 2000;26:93–104.

Uhlendorf V, Hoffman C. Nonlinear acoustic response of coated microbubbles in diagnostic ultrasound. Proceedings of the IEEE Ultrasound Symposium. Cannes, France, 1994;1559–1562.

Unger E, Shen DK, Fritz T, et al. Gas-filled lipid bilayers as ultrasound contrast agents. Invest Radiol 1994;29:S134–S136.